

## Topological Insulating in GeTe/Sb<sub>2</sub>Te<sub>3</sub> Phase-Change Superlattice

Baisheng Sa,<sup>1,4</sup> Jian Zhou,<sup>1</sup> Zhimei Sun,<sup>1,2,\*</sup> Junji Tominaga,<sup>3</sup> and Rajeev Ahuja<sup>4</sup>

<sup>1</sup>Department of Materials Science and Engineering, College of Materials, Xiamen University, 361005 Xiamen, China

<sup>2</sup>Fujian Provincial Key Laboratory of Theoretical and Computational Chemistry (Xiamen University), 361005 Xiamen, China

<sup>3</sup>Green Nanoelectronics Center, National Institute of Advanced Industrial Science and Technology (AIST), Tsukuba Central 4, 1-1-1 Higashi, Tsukuba, 305-8562, Japan

<sup>4</sup>Department of Physics and Astronomy, Uppsala University, 75120 Uppsala, Sweden, and Department of Materials and Engineering, Royal Institute of Technology, 10044 Stockholm, Sweden

(Received 13 April 2012; published 30 August 2012)

GeTe/Sb<sub>2</sub>Te<sub>3</sub> superlattice phase-change memory devices demonstrated greatly improved performance over that of Ge<sub>2</sub>Sb<sub>2</sub>Te<sub>5</sub>, a prototype record media for phase-change random access memory. In this work, we show that this type of GeTe/Sb<sub>2</sub>Te<sub>3</sub> superlattice exhibits topological insulating behavior on the basis of *ab initio* calculations. The analysis of the band structures and parities as well as  $Z_2$  topological invariants unravels the topological insulating nature in these artificial materials. Furthermore, the topological insulating character remains in the GeTe/Sb<sub>2</sub>Te<sub>3</sub> superlattice under small compressive strains, whereas it is not observed as more Sb<sub>2</sub>Te<sub>3</sub> building blocks introduced in the superlattice. The present results show that multifunctional data storages may be achieved in the GeTe/Sb<sub>2</sub>Te<sub>3</sub> superlattice. Such kinds of artificial materials can be used in phase-change random access memory, spintronics, and quantum computing.

DOI: [10.1103/PhysRevLett.109.096802](https://doi.org/10.1103/PhysRevLett.109.096802)

PACS numbers: 73.20.At, 71.15.Dx, 71.18.+y, 71.20.Nr

Putting two types of crystals together in one lattice creates a superlattice with properties different from or greater than the sum of those of its individual components. For example, neither SrCuO<sub>2</sub> nor BaCuO<sub>2</sub> is a superconductor, whereas a superlattice consisting of thin layers of both oxides exhibits superconducting behavior [1]; a three-component ferroelectric BaTiO<sub>3</sub>/SrTiO<sub>3</sub>/CaTiO<sub>3</sub> superlattice has 50% enhancement in ferroelectric polarization compared with its only ferroelectric component, barium titanate [2]. Recently, the property enhancement has been achieved in a two-component phase-change GeTe/Sb<sub>2</sub>Te<sub>3</sub> superlattice, also referred as interfacial phase-change materials (IPCM) by Simpson *et al.* [3]. Chalcogenide phase-change materials are widely investigated to replace Flash memory for the application of nonvolatile data storage [4], which relies on the large contrast in electrical or optical properties between the amorphous and crystalline states of the phase-change materials switched reversibly by heat pulses [5]. Among the chalcogenides, Ge<sub>2</sub>Sb<sub>2</sub>Te<sub>5</sub> (GST) in the GeTe-Sb<sub>2</sub>Te<sub>3</sub> tie line exhibits the best performance in terms of speed and scalability [6], whereas compared to GST, the IPCM data storage devices exhibit dramatically improved performance in terms of reduced switching energies, improved write-erase cycle lifetimes, and faster switching speeds [3]. Furthermore, an extraordinarily large magnetoresistance of  $\Delta R/R > 2000\%$  has been reported in the GeTe/Sb<sub>2</sub>Te<sub>3</sub> superlattice, which is induced by applying an electrical field at temperatures exceeding 400 K [7]. Therefore, Tominaga *et al.* believed that the results paves the way for developing conceptually new memory devices combining the merits of both phase-change memory and magnetic data storage [7].

On the other hand, trigonal GST has also been shown to exhibit topological insulating behavior either at ambient conditions or induced by hydrostatic pressures or mechanical strains [8–10]. In addition, Sb<sub>2</sub>Te<sub>3</sub> was reported to be a topological insulator (TI) with a conducting surface state [11]. It is thus natural to speculate that the GeTe/Sb<sub>2</sub>Te<sub>3</sub> superlattice could also exhibit topological insulating behavior. At the European Phase Change and Ovonic Symposium 2011, Tominaga *et al.* once mentioned that IPCM could be a TI merely based on the presence of a strong Rashba effect [12]. However, both experimental and theoretical realization that IPCM is a TI is lacking. In this Letter, we unravel the topological insulating nature of GeTe/Sb<sub>2</sub>Te<sub>3</sub> superlattices based on *ab initio* calculations. The present work expands not only the catalog of TIs but also the applications of GeTe/Sb<sub>2</sub>Te<sub>3</sub> superlattice phase-change materials. These remarkable superlattices will find their applications in phase-change random access memory, spintronics, and quantum computing, and hence multifunctional data storage can be achieved.

Our theoretical calculations are based on density functional theory (DFT) within generalized gradient approximations of Perdew-Burke-Ernzerhof (PBE) in conjunction with projector augmented wave (PAW) potentials which is implemented in the Vienna *ab initio* simulation package (VASP) [13]. The calculation details are given in Supplemental Material [14]. To have a direct comparison with Ge<sub>2</sub>Sb<sub>2</sub>Te<sub>5</sub>, the prototype, and well investigated phase-change material, we first studied the TI behavior of the [(GeTe)<sub>2</sub>(Sb<sub>2</sub>Te<sub>3</sub>)<sub>1</sub>] superlattice. The crystal structures of the [(GeTe)<sub>2</sub>(Sb<sub>2</sub>Te<sub>3</sub>)<sub>1</sub>] superlattice were constructed from the ⟨001⟩ direction of trigonal Sb<sub>2</sub>Te<sub>3</sub> and the ⟨111⟩

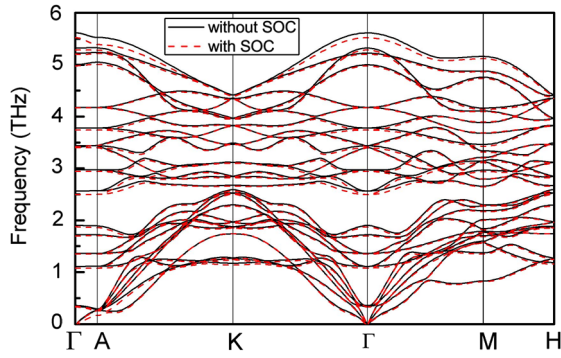


FIG. 1 (color online). Phonon dispersion curve for GTST without SOC and with SOC.

direction of cubic GeTe, with an atomic stacking of Te-Sb-Te-Te-Ge-Ge-Te-Te-Sb-, hereafter referred to as GTST [Fig. S1(a)] [14]. For comparison, the two typical stacking models for trigonal  $\text{Ge}_2\text{Sb}_2\text{Te}_5$  (GST) [15], referred to as GST-I [Fig. S1(b)] and GST-II [Fig. S1(c)], have also been studied.

Our PAW-PBE calculations show that GTST exhibits the same space group ( $P\bar{3}m1$ ) as trigonal GST, in agreement with previous work of IPCM [3]. GTST has smaller  $a$  but larger  $c$  parameters which results in a larger unit cell volume compared to GST-I and GST-II (Table S1). Furthermore, GTST is energetically stable by its lower cohesive energy than that of GST-II (Table S1). Our results provide a picture for GTST with a low density structure and high stability.

To further explore the lattice dynamic stability of GTST, we have calculated the phonon dispersions both without spin-orbit coupling (SOC) and with SOC as shown in Fig. 1. Obviously, there is no negative frequency observed for GTST either without SOC or with SOC, suggesting that GTST is dynamically stable. The good lattice dynamic stability of GTST agrees well with the above discussed energetic stability. Furthermore, the degenerate transverse acoustic mode calculated without SOC is lifted with SOC along the  $\Gamma$  (0, 0, 0) to A (0, 0, 0.5) direction, with one mode obviously lower than the other two. The result reveals the softening of the transverse acoustic mode in the  $\Gamma$  to A

direction. Hence the effect of SOC on the lattice and atomic vibrations in GTST is mainly along the  $c$  direction.

Table I lists the calculated bond lengths and charge transfers for the constitute elements of GTST, the results of which for GST-I and GST-II are given in Table S2 for comparison. The interaction between the adjacent Te atoms in GST has been argued to be van der Waals (vdW)-like weak bonding [16]. However, traditional exchange and correlation potentials like PBE can hardly treat such a weak interaction well. Therefore, in this work we have also performed DFT calculations with vdW corrections by the approach of Grimme [17] (DFT-D2) to understand the weak interaction in GTST. As seen in Table I, PBE provides larger lattice parameters and longer bond lengths than DFT-D2. The largest difference is observed in lattice parameter  $c$  as well as the Te-Te (0.361 Å difference) and Ge-Ge (0.106 Å difference) homopolar bonds. Meanwhile, the strong covalent Ge-Te and Sb-Te bonds are slightly affected by the calculation methods with the differences being within 0.05 Å. On the other hand, the bond length of Ge-Ge 2.958 Å is much larger than the ideal Ge-Ge covalent bond length 2.40 Å [18]. The Te-Te bond length in GTST is also larger than that in GST-I and GST-II (Table S2). The results indicate that the weak interaction between adjacent Te and Te and between adjacent Ge and Ge is vdW-type bonding. This vdW-type weak bonding is further confirmed by analyzing the charge density (Fig. S2) and charges on the Bader atoms (Table I) which are bound through a bond point [14]. This type of Ge-Ge weak bonding results in the easy movement of Ge atoms and thus can explain the proposed phase-change model of Ge atoms switching between tetrahedral and octahedral sites at the interfacial GeTe/Sb<sub>2</sub>Te<sub>3</sub> [3]. The charge transfer between the building units of GeTe and Sb<sub>2</sub>Te<sub>3</sub> in GTST superlattice can be viewed by the Bader charge analysis [19,20]. As seen in Table I, the ionic charges in GTST superlattice can be presented as  $\text{Ge}^{0.17+}\text{Te}^{0.18-}(\text{Sb}^{0.355+})_2(\text{Te}^{0.23-})_3$  and  $\text{Ge}^{0.25+}\text{Te}^{0.26-}(\text{Sb}^{0.52+})_2(\text{Te}^{0.34-})_3$  by PAW-PBE and DFT-D2 calculations, respectively. Even though the charge transfer around an individual element by the two methods is different, the ionic charges in GTST can be viewed as

TABLE I. The calculated lattice parameters and bond lengths as well as the Bader charge and volumes according to Bader analysis in GTST using the PBE and DFT-D2 methods.

	Lattice parameters (Å)					Bond length (Å)				
	$a$	$c$	Ge-Te <sub>3</sub>	Sb-Te <sub>1</sub>	Sb-Te <sub>2</sub>	Te <sub>3</sub> -Te <sub>3</sub>	Ge-Ge			
PBE	4.206	19.359	2.829	2.997	3.172	4.226	3.064			
DFT-D2	4.140	18.288	2.796	2.972	3.128	3.865	2.958			
	Bader charge $Q_B$ ( $e$ )					Bader volume $V_B$ (Å <sup>3</sup> )				
	Ge	Sb	Te <sub>1</sub>	Te <sub>2</sub>	Te <sub>3</sub>	Ge	Sb	Te <sub>1</sub>	Te <sub>2</sub>	Te <sub>3</sub>
PBE	3.83	4.64 <sub>5</sub> <sup>a</sup>	6.35	6.17	6.18	23.23	28.38	32.41	39.87	40.04
DFT-D2	3.75	4.48	6.42	6.30	6.26	20.77	25.36	32.26	37.15	36.31

<sup>a</sup>Note: The subscript 5 for Sb in Bader charge is the third digit after the decimal point.

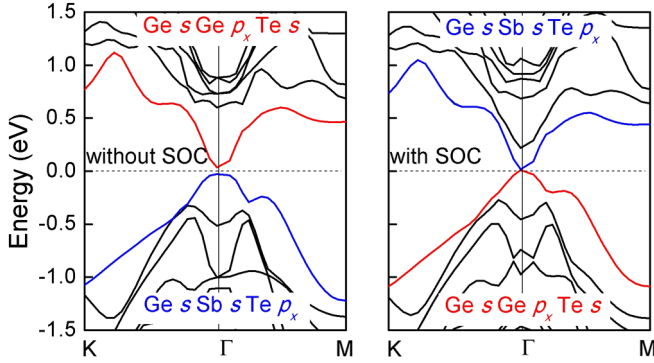


FIG. 2 (color online). Bulk band structures for GTST without SOC and with SOC.

$(\text{GeTe})^{0.01-}_2(\text{Sb}_2\text{Te}_3)^{0.02+}$ . It is clear that there are only  $0.02e$  charge transfers from  $\text{Sb}_2\text{Te}_3$  to  $\text{GeTe}$ . This tiny charge transfer together with the GTST superlattice configuration [Fig. S1(a)] reveals very weak interaction between the building units of  $\text{GeTe}$  and  $\text{Sb}_2\text{Te}_3$ . This weak interaction can be neglected and will not affect the topological nature of GTST.

The bulk band structures without and with SOC for GTST were plotted in Fig. 2. As seen in the figure, GTST is a narrow band gap (0.07 eV) semiconductor with a direct band gap at the  $\Gamma$  point without SOC. The conduction band minimum (CBM) at the  $\Gamma$  point is occupied by the  $\text{Ge } s \text{ Ge } p_x \text{ Te } s$  state, and the valence band maximum (VBM) at the  $\Gamma$  point is occupied by the  $\text{Ge } s \text{ Sb } s \text{ Te } p_x$  state. With introducing SOC, the electronic structure of GTST shows a very small band gap (0.01 eV) by inverting the band characterizations of CBM and VBM. For the observed tiny band gap, it is well known that DFT calculations always underestimate the band gap of a system. Fortunately, in this respect, the hybrid function with the mixing of the Hartree-Fock and DFT exchange terms is a practical solution to solve the band gap problem [21]. Therefore, we use the Heyd-Scuseria-Ernzerhof [22] hybrid functional to further investigate the band inversion of GTST. The calculated total electron density of states for GTST without SOC and with SOC is shown in Fig. S3 [14]. The band gap of GTST is 0.23 eV without SOC and is 0.12 eV with SOC, which is around 3 and 12 times that calculated by PBE, respectively. This band gap with SOC is very close to the newly discovered actinide TI materials [23]. Therefore, our results indicate a topological insulating nature in GTST [24].

As it has been shown previously that compressive strain can tune the topological nature of materials [25], we have applied 2% and 4% compressive strains along the  $c$  axis to GTST to study the effect of strain on the band inversion. The corresponding bulk band structures are illustrated in Figs. 3(a) and 3(b), where SOC induced  $\text{Ge } s \text{ Ge } p_x \text{ Te } s$  and  $\text{Ge } s \text{ Sb } s \text{ Te } p_x$  band inversion is clearly seen. Furthermore, the existence of small compressive strain in GTST results in the band overlap at the  $\Gamma$  point without SOC but induces the opening of a band gap with SOC. The results indicate that GTST could be a TI even under compressive

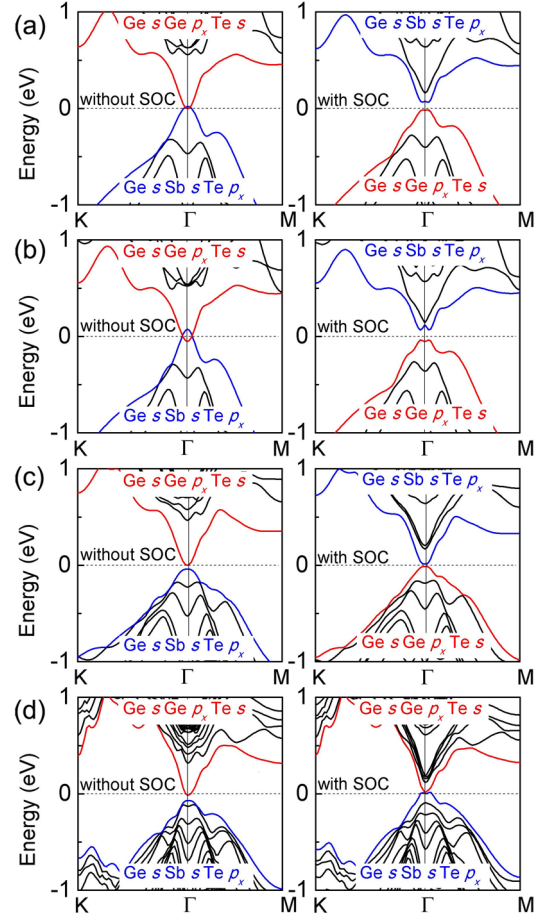


FIG. 3 (color online). Bulk band structures for GTST under (a) 2% and (b) 4% compressive strain along the  $c$  direction, (c)  $[(\text{GeTe})_2(\text{Sb}_2\text{Te}_3)_2]$ , and (d)  $[(\text{GeTe})_2(\text{Sb}_2\text{Te}_3)_4]$  without and with SOC. The Fermi level is set at 0 eV.

strains. It is also interesting to note that, for GTST under a 4% compressive strain, the time-reversal symmetry at the  $\Gamma$  point is invariant and two peaks around the  $\Gamma$  point in CBM reveal a strong Rashba effect.

To investigate the effect of stoichiometry or building blocks on the band inversion, we have considered two other superlattices, i.e.,  $[(\text{GeTe})_2(\text{Sb}_2\text{Te}_3)_2]$  and  $[(\text{GeTe})_2 \times (\text{Sb}_2\text{Te}_3)_4]$  with a stoichiometry of  $\text{Ge}_1\text{Sb}_2\text{Te}_4$  and  $\text{Ge}_1\text{Sb}_4\text{Te}_7$ , respectively. For  $[(\text{GeTe})_2(\text{Sb}_2\text{Te}_3)_2]$ , the Te-Ge-Ge-Te unit locates in between two  $\text{Sb}_2\text{Te}_3$  blocks, and it bisects four  $\text{Sb}_2\text{Te}_3$  blocks for  $[(\text{GeTe})_2(\text{Sb}_2\text{Te}_3)_4]$ . Figures 3(c) and 3(d) show the bulk band structures for  $[(\text{GeTe})_2(\text{Sb}_2\text{Te}_3)_2]$  and  $[(\text{GeTe})_2(\text{Sb}_2\text{Te}_3)_4]$ , respectively. It is seen that the SOC induced band inversion of VBM and CBM is observed in  $[(\text{GeTe})_2(\text{Sb}_2\text{Te}_3)_2]$  but not in  $[(\text{GeTe})_2(\text{Sb}_2\text{Te}_3)_4]$ . Obviously, the topological insulating nature of IPCM may be closely related to the geometry of the superlattice which will be further analyzed below.

It is known that the “Dirac cone” featured metallic surface state is the direct evidence of a TI [26,27]. We studied two important surfaces for GTST; i.e., one was constructed by

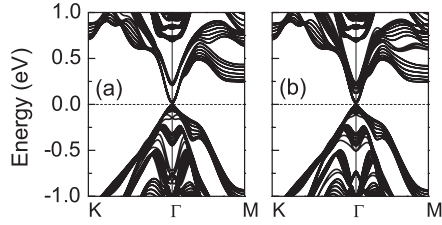


FIG. 4. The surface band structures for (a)  $S_{Te}$  and (b)  $S_{Ge}$  of GTST. The Fermi level is set at 0 eV.

cleaving the adjacent Te layers ( $S_{Te}$ -GTST), and the other was constructed by cleaving the adjacent Ge layers ( $S_{Ge}$ -GTST). More details about the surface constructions are given in Supplemental Material [14]. Figure 4 shows the surface band structure for the two fully relaxed surface atomic structures with SOC, where a Dirac cone feature at the  $\Gamma$  point is seen even though the node is hardly separated from the bulk conduction band. To further investigate the effect of vdW corrections on the band structure, we have also calculated the bulk band structure and surface band structure of  $S_{Te}$ -GTST by DFT-D2 methods, the results of which are illustrated in Fig. 5. Obviously, as seen in Fig. 5(a), the vdW correction increases the band gap of bulk band structure in contrast to the very small band gap obtained by PBE with SOC. Furthermore, the conducting surface state with a Dirac cone feature at the  $\Gamma$  point is distinguished from the bulk conduction band [Fig. 5(b)]. The present results clearly unravel the topological insulating nature of GTST.

Based on the above results, i.e., the band character inversion of VBM and CBM of the bulk band structure as well as the distinguished Dirac cone featured metallic surface state for the GTST superlattice, it is clear that the  $GeTe/Sb_2Te_3$  superlattice with a stoichiometric  $Ge_2Sb_2Te_5$  is a TI. In the following, we present a simple analysis on the topological insulating character of GTST. It has been shown that the most general and direct approach to understand a TI with inversion symmetry is to analyze the  $Z_2$  topological invariants from the parities of time-reversal invariant moments [28]. The calculation details of the  $Z_2$  topological invariants  $\nu_0;(\nu_1\nu_2\nu_3)$  [29] are given in Supplemental Material [14]. The products of the parities

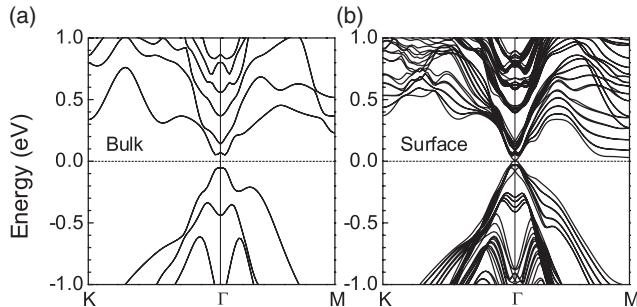


FIG. 5. The GTST bulk and  $S_{Te}$ -GTST surface band structure with SOC using the DFT-D2 method. The Fermi level is set to 0 eV.

for the occupied bands of  $[(GeTe)_2(Sb_2Te_3)_1]$  (GTST),  $[(GeTe)_2(Sb_2Te_3)_2]$ , and  $[(GeTe)_2(Sb_2Te_3)_4]$  are given in Table S3, S4, and S5, respectively. The corresponding calculated  $Z_2$  topological invariants  $\nu_0;(\nu_1\nu_2\nu_3)$  are 1; (110), 1;(001) and 0;(000), which verifies that GTST and  $[(GeTe)_2(Sb_2Te_3)_2]$  are strong TIs while  $[(GeTe)_2 \times (Sb_2Te_3)_4]$  is a normal semiconductor. These results agree well with the above analysis on the band inversions. Furthermore, the results show that the topological insulating nature will disappear with the increase in the content of  $Sb_2Te_3$ , suggesting that the Te-Ge-Ge-Te building unit plays a very important role in the topological insulating properties of GTST.

The band inversion of VBM and CBM in trigonal  $Ge_2Sb_2Te_5$  has been characterized to be the inversion of the Ge  $s$  Sb  $s$  states with Ge  $p$  Sb  $p$  states under SOC for GST-I [9,10] and the inversion of Te  $s$  states with Te  $p$  states under SOC for GST-II [9], whereas for the GTST superlattice, the band inversion was characterized to be the inversion of the Ge  $s$  Ge  $p_x$  Te  $s$  state with the Ge  $s$  Sb  $s$  Te  $p_x$  state under SOC. It is obvious that the topological insulating character in the  $GeTe/Sb_2Te_3$  superlattice results from the special atomic configuration, particularly the directly bonded Ge-Ge weak bonds. For this strong Rashba effect in IPCM [7], Tominaga *et al.* observed that if a displacement of the second Sb due to the interfacial stress from a lattice mismatch happens, it has the potential to induce a large Rashba effect by the break of the spatial symmetry, while the present results show that the  $GeTe/Sb_2Te_3$  superlattice is a TI at ambient conditions when there are directly weak Ge-Ge bond. On the other hand, the weakly bonded adjacent Ge atoms may be the origin of the easy switch of these special Ge atoms between tetrahedral and octahedral positions to which was attributed the origin of phase-change data storage in IPCM by Simpson *et al.* [3]. Therefore, multifunctional data storage devices that combine the merits of both phase-change memory and quantum computing can be achieved in  $GeTe/Sb_2Te_3$  superlattices. Furthermore, the previously reported phenomenon of electrical-field induced giant magnetoresistivity in  $GeTe/Sb_2Te_3$  superlattices indicates that it is possible to develop conceptually new memory devices that combine the merits of phase-change memory, magnetic data storage, and quantum computing. The present findings open new insights on tailoring phase-change materials and the performance of data storage devices.

In conclusion, we have investigated the topological insulating behavior in  $GeTe/Sb_2Te_3$  superlattices by means of *ab initio* calculations. Using  $[(GeTe)_2(Sb_2Te_3)_1]$  as an example, we show that this artificial material is dynamically stable based on the phonon dispersion analysis and is a TI as analyzed by the band structures and parities as well as  $Z_2$  invariants. Furthermore, the topological insulating character is also observed even under small compressive strains. However, with further increasing the number of  $Sb_2Te_3$  blocks to  $[(GeTe)_2(Sb_2Te_3)_4]$ , the superlattice remains as

a normal semiconductor. As TIs have great potential applications in quantum computing [30], the present work shows that developing a new conceptual memory device that combines the merits of both quantum computing and phase-change data storage is possible.

This work is supported by National Natural Science Foundation of China (60976005), the Outstanding Young Scientists Foundation of Fujian Province of China (2010J06018) and the Fundamental Research Funds for the Central Universities (2010121054). The study of B. S. at Sweden is supported by China Scholarship Council (CSC). R. A. thanks VR for financial support.

---

\*To whom all correspondence should be addressed.  
zmsun@xmu.edu.cn; zhmsun2@yahoo.com

- [1] D. P. Norton, B. C. Chakoumakos, J. D. Budai, D. H. Lowndes, B. C. Sales, J. R. Thompson, and D. K. Christen, *Science* **265**, 2074 (1994).
- [2] H. N. Lee, H. M. Christen, M. F. Chisholm, C. M. Rouleau, and D. H. Lowndes, *Nature (London)* **433**, 395 (2005).
- [3] R. E. Simpson, P. Fons, A. V. Kolobov, T. Fukaya, M. Krbal, T. Yagi, and J. Tominaga, *Nature Nanotech.* **6**, 501 (2011).
- [4] A. V. Kolobov, *Nature Mater.* **7**, 351 (2008).
- [5] Z. Sun, J. Zhou, Y. Pan, Z. Song, H.-K. Mao, and R. Ahuja, *Proc. Natl. Acad. Sci. U.S.A.* **108**, 10410 (2011).
- [6] D. Lencer, M. Salinga, B. Grabowski, T. Hickel, J. Neugebauer, and M. Wuttig, *Nature Mater.* **7**, 972 (2008).
- [7] J. Tominaga, R. E. Simpson, P. Fons, and A. V. Kolobov, *Appl. Phys. Lett.* **99**, 152105 (2011).
- [8] J. Kim, J. Kim, and S.-H. Jhi, *Phys. Rev. B* **82**, 201312 (2010).
- [9] B. S. Sa, J. Zhou, Z. T. Song, Z. M. Sun, and R. Ahuja, *Phys. Rev. B* **84**, 085130 (2011).
- [10] B. S. Sa, J. Zhou, Z. M. Sun, and R. Ahuja, *Europhys. Lett.* **97**, 27003 (2012).
- [11] H. Zhang, C.-X. Liu, X.-L. Qi, X. Dai, Z. Fang, and S.-C. Zhang, *Nature Phys.* **5**, 438 (2009).
- [12] J. Tominaga, P. J. Fons, M. Hase, and A. V. Kolobov, in *Proceedings of the European Phase Change and Ovonic Symposium, 2011* (unpublished), p. 26.
- [13] J. Hafner, *J. Comput. Chem.* **29**, 2044 (2008).
- [14] See Supplemental Material at <http://link.aps.org/supplemental/10.1103/PhysRevLett.109.096802> for the computational details and additional results and discussions.
- [15] Z. M. Sun, J. Zhou, and R. Ahuja, *Phys. Rev. Lett.* **96**, 055507 (2006).
- [16] B. S. Sa, N. H. Miao, J. Zhou, Z. M. Sun, and R. Ahuja, *Phys. Chem. Chem. Phys.* **12**, 1585 (2010).
- [17] S. Grimme, *J. Comput. Chem.* **27**, 1787 (2006).
- [18] B. Cordero, V. Gómez, A. E. Platero-Prats, M. Revés, J. Echeverría, E. Cremades, F. Barragán, and S. Alvarez, *Dalton Trans.* (2008) 2832.
- [19] E. Sanville, S. D. Kenny, R. Smith, and G. Henkelman, *J. Comput. Chem.* **28**, 899 (2007).
- [20] W. Tang, E. Sanville, and G. Henkelman, *J. Phys. Condens. Matter* **21**, 084204 (2009).
- [21] J. Muscat, A. Wander, and N. M. Harrison, *Chem. Phys. Lett.* **342**, 397 (2001).
- [22] J. Paier, M. Marsman, K. Hummer, G. Kresse, I. C. Gerber, and J. G. Ángyán, *J. Chem. Phys.* **124**, 154709 (2006).
- [23] X. Zhang, H. Zhang, J. Wang, C. Felser, and S.-C. Zhang, *Science* **335**, 1464 (2012).
- [24] S. Chen, X. G. Gong, C.-G. Duan, Z.-Q. Zhu, J.-H. Chu, A. Walsh, Y.-G. Yao, J. Ma, and S.-H. Wei, *Phys. Rev. B* **83**, 245202 (2011).
- [25] W. Liu, X. Peng, C. Tang, L. Sun, K. Zhang, and J. Zhong, *Phys. Rev. B* **84**, 245105 (2011).
- [26] M. Z. Hasan and C. L. Kane, *Rev. Mod. Phys.* **82**, 3045 (2010).
- [27] X.-L. Qi and S.-C. Zhang, *Rev. Mod. Phys.* **83**, 1057 (2011).
- [28] C. L. Kane and E. J. Mele, *Phys. Rev. Lett.* **95**, 146802 (2005).
- [29] L. Fu and C. L. Kane, *Phys. Rev. B* **76**, 045302 (2007).
- [30] J. E. Moore, *Nature (London)* **464**, 194 (2010).